MicroRNA-495 Inhibits New Bone Regeneration via Targeting High Mobility Group AT-Hook 2 (HMGA2)

Authors' Contribution:
Study Design A
Data Collection B
Statistical Analysis C
Data Interpretation D
Manuscript Preparation E
Literature Search F
Funds Collection G

BE Zhao Tian*
B Haizhen Zhou*
CD Yuben Xu
A Jie Bai

Department of Hand Surgery, Honghui Hospital, Xi'an Jiaotong University College of Medicine, Xi'an, Shaanxi, P.R. China

Corresponding Author: * Equal contributors
Jie Bai, e-mail: Baijiedoctor@163.com
Source of support: Departmental sources

Background: MicroRNAs play critical roles in post-translational gene expression. In this study, we explored the role of miR-495 in new bone regeneration.

Material/Methods: Murine calvarial osteoblasts were isolated and cultured. Microarray was performed to identify differential miR-NAs in medicarpin-induced osteoblasts differentiation. Luciferase reporter assay was performed to identify the target gene of miRNA. Murine osteoblast cells were transfected with miC, miR-495, or anti-miR-495. CCK-8 and flow cytometry were performed to detect osteoblasts proliferation and apoptosis. Western blot was used to analyze apoptosis-related proteins. qRT-PCR analysis was performed to detect gene expression. ALP activity and mineralized nodule formation test were used to evaluate bone formation. Dill-hole injury model was constructed and micro CT was utilized to measuring bone healing.

Results: Microarray analysis identified miR-495 as our miRNA of interest and luciferase reporter assay identified HMGA2 as its target gene. Over-expression of miR-495 significantly inhibited ALP activity and mineralized nodule formation as well as the expression of RUNX-2, BMP-2, and Osterix. Also, miR-495 over-expression inhibited osteoblasts proliferation and promoted apoptosis obviously. In this *in vivo* study, the downregulation of miR-495 promoted murine femur healing.

Conclusions: MiR-495 inhibits new bone regeneration via targeting high mobility group AT-Hook 2 (HMGA2). We propose that targeting miR-495 may be a promising therapeutic approach for bone regeneration.

MeSH Keywords: **Bone Regeneration • HMGA2 Protein • Microarray Analysis • MicroRNAs**

Full-text PDF: https://www.medscimonit.com/abstract/index/idArt/904404

📄 2527   ▦ —   📊 5   📑 32

Background

MicroRNAs (miRNAs) are a cluster of small (about 22 nucleo-tides), noncoding and single-stranded RNAs which were highly conserved in plants, animals, and even some viruses, and they regulates gene expression post-translationally [1–3]. MiRNAs function via partial or complete base-paring with complementary sequences within mRNA molecules [4,5]. The dysregulation of miRNAs is associated with a number of diseases. It was reported that mutations of miRNAs could be found in some inherited diseases such as progressive hereditary hearing loss [6], hereditary keratoconus with anterior polar cataract [7], and skeletal and growth defects [8]. In recent years, an increasing number of miRNAs have been found to be linked with cancers. For example, low levels of miR-324a could serve as an indicator of poor survival [9]. In addition, some specific miR-NAs have been associated with certain histological subtypes of colorectal cancer [10]. Also, miRNAs participate in heart development [11], and cholesterol metabolism and regulation [12].

A growing number of studies have revealed that miRNAs also regulate osteoblasts differentiation, bone metabolism, and bone formation. MiR-467g negatively regulates osteogenesis by targeting Ihh(Indian hedgehog)/Runx-2 (runt-related transcription factor 2) signaling pathway [13]. MiR-221 inhibits osteoblasts differentiation and bone formation directly by targeting RUNX2 in osteoporosis models [14]. MiR-214 suppresses osteogenesis by targeting BIRC7 (baculoviral IAP repeat-containing 7) [15]. During the process of cyclical stretch-induced bone formation, miR-503-5p inhibits bone mesenchymal stem cells (BMSCs) osteogenic differentiation and bone formation functioning as a mechanosensitive miRNA [16]. Thus, miRNAs may progressed as novel therapeutic targets for the treatment of bone degenerative disorders and other abnormal bone formation diseases.

Medicarpin was reported to promote osteoblast differentiation via ER-BMP-2 signaling pathway which deregulates diverse miRNAs [17]. We deduced that miRNAs may play a role in the process of medicarpin-induced osteogenesis. To screen miRNAs changes in osteogenesis, we performed microarray analysis and found that several miRNAs were downregulated. Among those candidates, we selected a markedly downregulated miR-495 as our target. In this study, we revealed that miR-495 inhibited osteoblast differentiation and new bone regeneration. The inhibition of miR-495 stimulated osteoblasts proliferation and differentiation *in vitro* and *in vivo*. MiR-495 suppressed bone formation directly by targeting HMGA2. Our results identified a novel miRNA in the regulation of osteoblast proliferation and bone regeneration.

Material and Methods

Isolation and culture of mice calvarial osteoblasts

First, one to two day old mice were sacrificed and their calvariae were removed. Calvariae were digested sequentially [18]. Briefly, calvariae were subjected to five sequential digestions at 37°C in 0.1% dispase and 0.1% collagenase P solution and cells were collected, centrifuged and resuspended in α-MEM medium supplemented with fetal bovine serum (10%) as well as 1% antibiotics.

Cell proliferation assay

Transfected osteoblast cells were plated in 96-well plates at a density of 5×10^3 cells per well. Then 48 hours later, 100 μL RPMI-1640 medium mixed with 10 μL CCK-8 solution was added to each well. After incubation at 37°C for 30 minutes, the absorbance of each well was detected at 450 nm. The analysis was repeated at least three times.

Microarray and miRNA target site prediction

Briefly, a total of 100 ng RNA was dephosphorylated and denatured. Then T4 ligase was used to ligate the cyanine-3-pCp and the 3' end of RNAs which were dephosphorylated. The mouse miRNA microarrays (8×15 K) were hybridized with labeled miRNA. After being washed sequentially, slides were promptly scanned with microarray scanner at 5 μm. Finally, the scanned images were quantified with Feature Extraction software and differentially expressed miRNAs were recognized. For the differentially expressed miRNAs, we utilized miRanda (*http://www.microrna.org*) and Target Scan (*http://www.targetscan.org*) to find promising target genes.

qRT-PCR analysis

We purchased TaqMan miRNA reverse transcription kit from Applied Biosystems to detect miR-495. Total RNAs were extracted from mice calvarial osteoblasts with TRIzol and reverse transcribed to get cDNAs. TaqMan Universal PCR Master Mix with MicroRNA Assay Mix together with cDNAs were mixed together and synthesized for DNAs with the Step One plus Real Time PCR systems. U6 was used as an internal control. Total RNAs were extracted from cells and reversed transcribed for cDNAs. The relative mRNA levels of RUNX-2, BMP-2, and Osterix were evaluated with GAPDH as an internal reference. These following primers were used:
U6 (forward: 5'-AGAGAAGAT TAGCATGGCCCCTG-3',
reverse: 5'-ATCCAGTGCAGGGTCCGAGG-3');
HMGA2 (forward: 5'–TCCCTCTAAAGCAGCTCAAAA-3',
reverse: 5'-ACTTGTTGTGGCCATTTCCT-3');
RUNX-2 (forward: 5'-GATGATGACACTGCCACCTCT-3',

reverse: 5'-AGGGCCCAGTTCTGAAGC-3');
BMP-2 (forward: 5'-CGGACTGCGGTCTCCTAA-3',
reverse: 5'- GGGGAAGCAGCAACACTAGA-3');
Osterix (forward: 5'- AGAGATCTGAGCTGGGTAGAGG-3',
reverse: 5'-AAGAGAGCCTGGCAAGAGG-3');
GAPDH (forward: 5'-AGCTTGTCATCAACGGGAAG-3',
reverse: 5'-TTTGATGTTAGTGGGGTCTCG-3').

For miRNA PCR analysis, the reaction mixtures were incubated in a 96 well plate at 95°C for 10 minutes followed by 40 cycles of 95°C for 15 seconds and at 60°C for one minute using the Step One plus Real-Time PCR system (Applied Biosystems). For osteogenic marker PCR analysis, the temperature profile of the reaction was 95°C for five minutes, 40 cycles of denaturation at 94°C for 2 minutes and annealing and extension at 62°C for 30 second, extension at 72°C for 30 seconds.

Transfection assay and ALP measurement

As osteoblasts reached a 50% confluence, miR-495 mimics and miRNA negative control were transfected with Oligofectamine. ALP activity and its mRNA level were detected after cells were transfected for 48 hours. Transfected cells were seeded in 96-well plates and cultured in medium supplied with β-glycerophosphate and ascorbic acid and then incubated for 48 hours. ALP activity was measured with p-nitrophenylphosphate as substrate after induction and detected for colorimetry at 405 nm.

Mineralization nodules formation assay

Cells were plated in differentiation medium supplemented with 10% FBS. Transfected cells were cultured for 21 days and medium changed every 48 hours. Then, after 21 days, cells were fixed with 4% formaldehyde and rinsed with PBS. Alizarin red-S was used to stain cells, with the nascent calcium stained. Then 10% acetic acid was added to the cells and cells were incubated for half an hour at room temperature. After incubation, cells were scraped, transferred to 1.5 mL tubes, and vortexed. Mineral oil purchased from Sigma-Aldrich was added to overlay the slurry and then the mix was heated, and centrifuged; 500 μl supernatant was collected and ammonium hydroxide added to neutralize the acid. The absorbance of supernatant was measured at 405 nm to analyze mineralization.

Luciferase reporter assay

Luciferase reporter assay was performed according to published protocols [19]. After osteoblast cells reached about 90%, pE-ZX-MT01 vector was transfected to osteoblast cells where wild or mutant types of 3'UTR of HMGA2 were cloned in special medium (reduced serum and antibiotics-free OptiMEM) supplemented with Oligofectamine 2000 for six hours. Firefly luciferase was the reporter gene and Renilla luciferase was the

tracking gene. In addition, miR-495 mimics or negative control was transfected to cells. Then, 48 hours later, the strength of luciferase and Renilla were detected in cell lysates by a Dual Luciferase Reporter Assay kit (Promega).

Drill-hole injury in femur

Six- to seven-week old female Balb/c mice were divided into two groups (n=8). All mice underwent drill-hole injury. Briefly speaking, the front skin in the femur diaphysis region was incised longitudinally for 1 cm under anesthetic conditions. After exposing the femoral surface, a 0.8 mm drill hole was made 2 cm above the knee joint. The two groups were drill-hole injury+miC and drill hole injury+anti-miR-495. After treatment for 21 days, all mice were sacrificed to collect femurs to measure bone micro architectural parameters at injury sites.

Microcomputed tomography analysis

SkyScan 1076micro CT scanner was used to collect bone parameters. The collected femurs were cleaned of soft tissues and muscles and scanned at 70 kV, 100 mA. Then SkyScan NRecon software was utilized for reconstruct images. Microarchitectural parameters including bone volume fraction (BV/TV), thickness of trabecularized spicules (Tb.Th), and trabecular number (Tb.N) were assessed.

Western blot assay

After washing with ice-cold PBS, transfected cells were lysed with PIPA buffer (Beyotime) to get total protein. We determined protein concentration with a protein assay kit; 10% SDS-PAGE was used to separate protein, and the samples were applied to PVDF membranes purchased from Millipore. Then 5% fat-free milk in TBST buffer was used to block non-specific protein interactions. The membranes were then incubated at 4°C with primary antibody for two hours; then incubated at room temperature with secondary antibody conjugated with horseradish peroxidase for two hours. After washing these membranes in TBST buffer, we developed the membranes using chemiluminescence to detect antibody concentrations and used β-actin as our internal control. The antibodies, anti-Bax, anti-Bcl-xl, and anti-β-actin were purchased from Abcam.

Apoptosis analysis

Cells were grown to about 50% confluence and exposed to miRC, miR-495, and anti-miR-495 for 24 hours. Annexin V-PI apoptosis kit was used to detect the apoptotic cells according to the manufacturer's instructions.
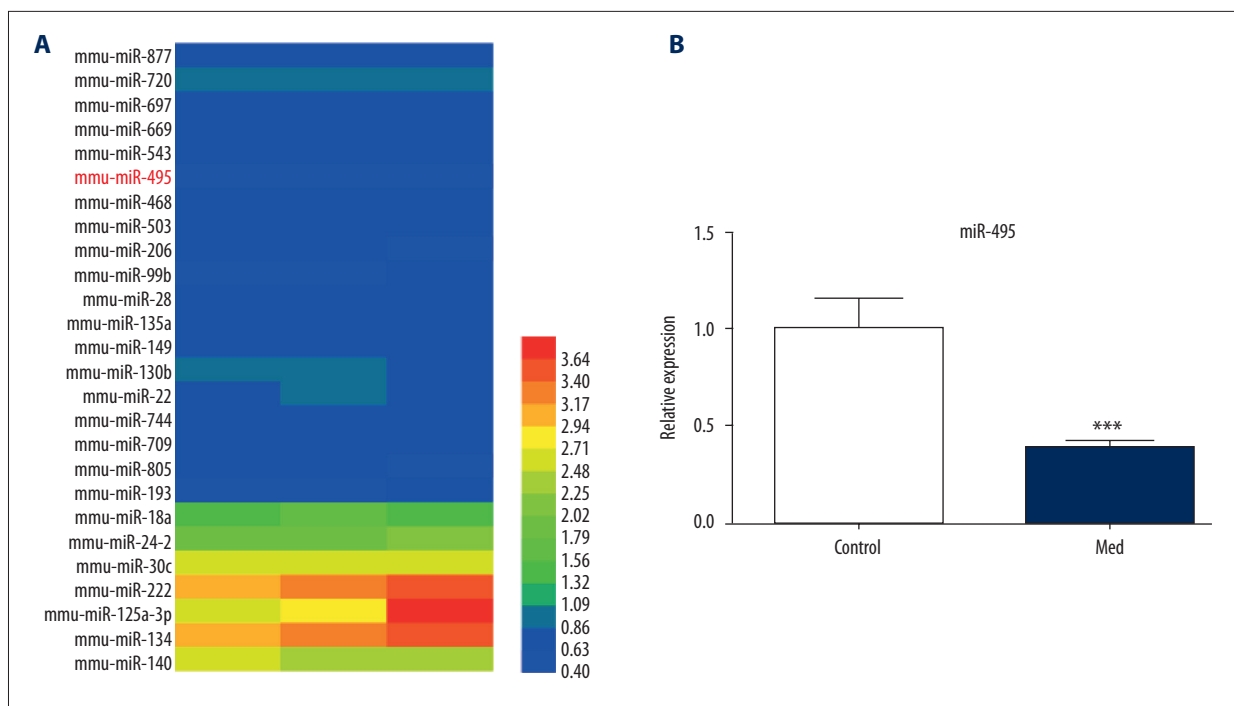
Figure 1. Selection of miRNAs of interest during medicarpin-induced osteogenesis. (**A**) miRNA array expression profiling. Red denotes high expression and blue denotes low expression relative to the control group. Only significantly upregulated and downregulated miRNAs are shown. (**B**) miR-495 expression during med-induced osteoblast differentiation. All values represent means of three independent experiments. *** $p<0.001$.

Statistical analysis

SPSS11.0 was used to analyze our data. Quantitative data was expressed as mean ±SD. Non-paired t-test was used to analyzed data between groups. The data obtained in experiments with multiple treatments were subjected to one-way ANOVA. A $p<0.05$ was determined as statistically significant.

Results

Selection of interesting miRNAs during medicarpin-induced osteogenesis

Medicarpin has been reported to induce osteoblasts differentiation definitely [17]. Therefore, we used medicarpin as an osteogenesis inducer to explore miRNAs differential expression in medicarpin-induced osteogenesis. Microarray analysis was performed on cells treated with or without medicarpin for 48 hours. Results from the microarray showed that most miRNAs were downregulated while a few were upregulated. We selected miR-495 as our miRNA of interest because it was significantly downregulated (Figure 1A). Furthermore, qRT-PCR analysis verified its downregulation in mice osteoblast cells (Figure 1B).

MiR-495 suppresses osteoblast differentiation

Osteoblasts were transfected with miR-C, mimic miR-495, and anti-miR-495 to evaluate the influence of miR-495 on osteoblast cells differentiation. We measured ALP activity, which is a common osteoblast cells differentiation marker. In miR-495 transfected cells, ALP activity was downregulated obviously while this effect was reversed in the inhibition group compared with cells transfected with miR-C (Figure 2A). In accordance with this effect, miR-495 decreased osteoblasts mineralized nodule formation, whereas this effect was blocked in the anti-miR-495 group (Figure 2B). Expression of osteogenic genes like RUNX-2, BMP-2, and Osterix were inhibited in the miR-495 group (Figure 2C), while this effect was reversed in the anti-miR-495 group. These results indicated that miR-495 suppressed osteoblast cell differentiation.

MiR-495 targets HMGA2 directly

To clarify the mechanisms of miR-495 suppressing osteoblast differentiation, miRanda (*http://www.microrna.org*) and Target Scan (*http://www.targetscan.org*) were utilized to identify promising target genes of miR-495. In particular, HMGA2 was a concern among those potential targets, as it has been reported that miR-33-5p promotes osteoblast differentiation by targeting HMGA2 [20]. Also, HMGA2 is associated with highly
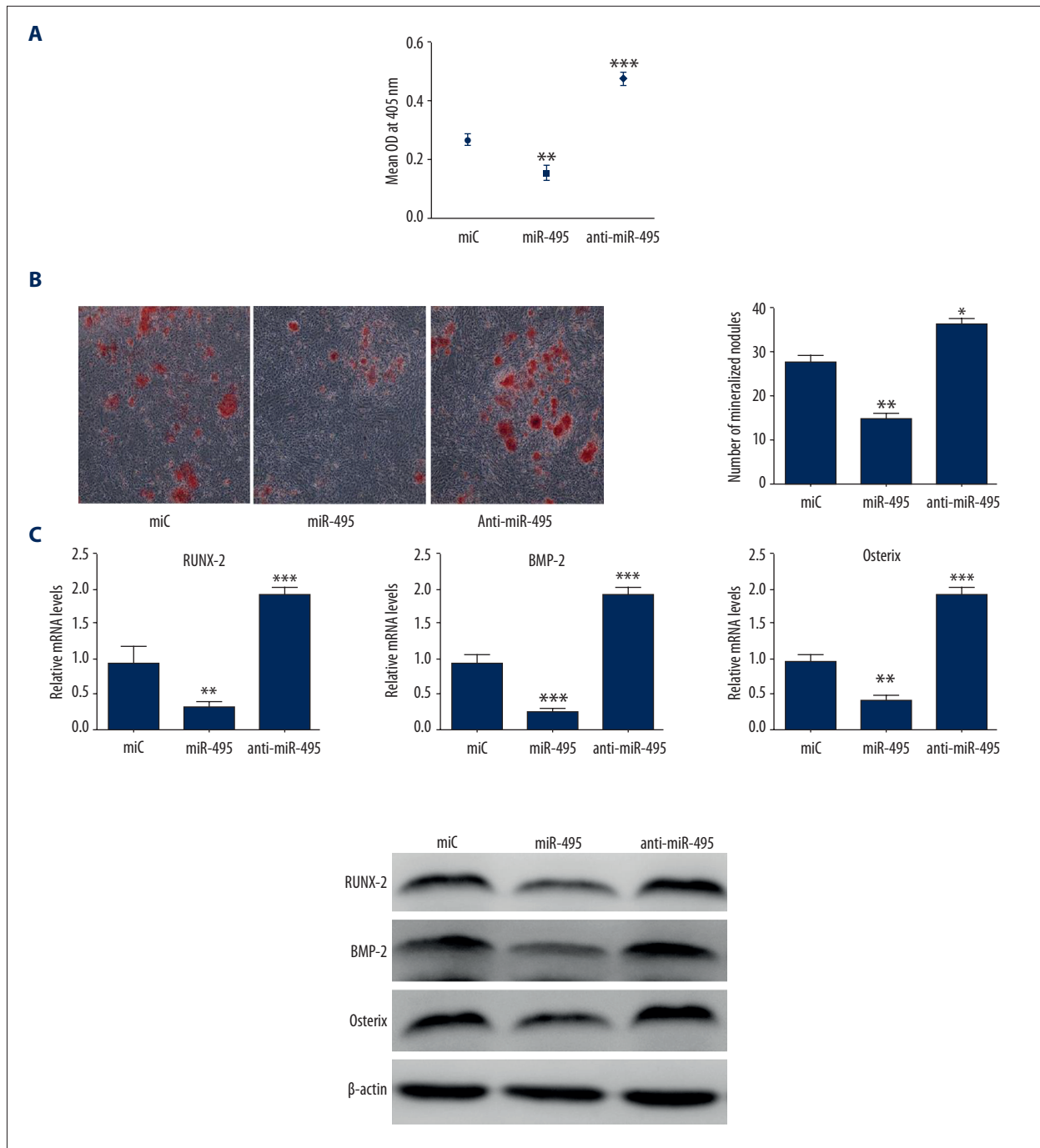
Figure 2. MiR-495 negatively regulates osteoblast differentiation. (**A**) Murine calvarial osteoblasts were transfected with miC, miR-495, and anti-miR-495 for 48 hours in differentiation medium. ALP activity in osteoblasts was measured. (**B**) Transfected murine osteoblasts were seeded in 12-well plates and stained with Alizarin red-S. Representative images show mineralized nodules in different groups. (**C**) qRT-PCR and Western blot analysis of osteoblast marker genes such as RUNX-2, BMP-2, and Osterix at 48 hours. * $p < 0.05$; ** $p < 0.01$; *** $p < 0.001$.
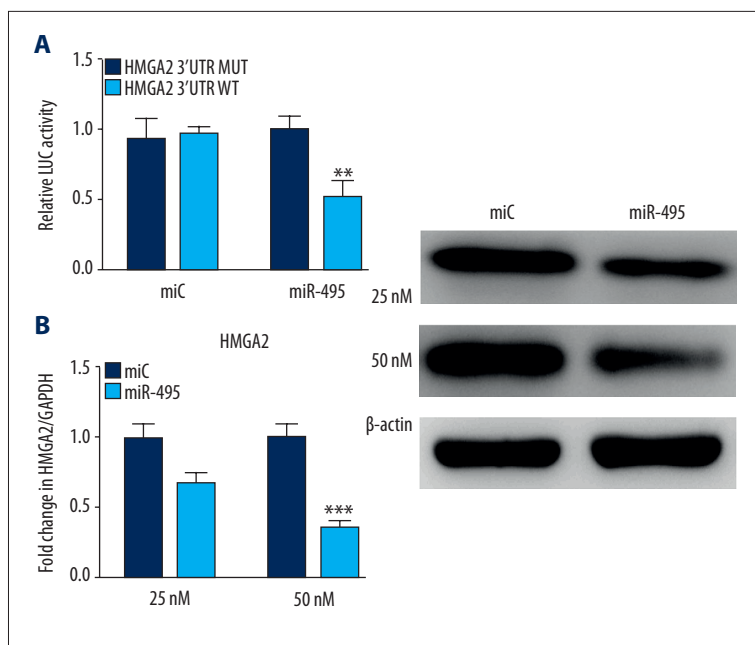

Figure 3. Identification of miR-495 target genes in osteoblast differentiation. (**A**) Effect of miR-495 over-expression on a dual luciferase reporter plasmid containing the HMGA2-3' UTR was analyzed. Cells were co-transfected with either the WT-pEZX MT01-HMGA2 or MUT-pEZX MT01-HMGA2 or an empty vector and miR-495 or miC. Firefly and Renilla luciferases were measured in cell lysate. (**B**) Cells were transfected with the miR-495 expression plasmid or a control. qRT-PCR and Western blot analysis for HMGA2 expression was performed. * $p<0.05$; ** $p<0.01$; *** $p<0.001$.

proliferating human bone marrow-derived mesenchymal stem cells and plays a role in bone formation [21]. Therefore, we selected HMGA2 as our target of interest. According to the prediction tools, 3'UTR of HMGA2 is the target of miR-495. We used luciferase reporter construct, involving the 3'UTR and mutations in the site of HMGA2, to test whether miR-495 could regulate HMGA2 directly. The expression vectors of mutant and wild HMGA2 were transfected with miR-495 mimics in osteoblasts and then the luciferase activity was detected. The reporter gene's luciferase activity was suppressed by over-expression of miR-495 while the suppression effect was abolished by mutations in the miRNA binding site (Figure 3A). To further directly verify this target, mice osteoblast was transfected with mimic miR-495, and qRT-PCR revealed the downregulated HMGA2 mRNA levels compared to the control group (Figure 3B).

MiR-495 over-expression inhibits proliferation and induces apoptosis of osteoblast by targeting HMGA2

CCK-8 assay was performed to test the influence of miR-495 on osteoblasts proliferation. Cells transfected with mimic miR-495 were inhibited proliferation compared with the control group (Figure 4A). However, we did not detect a significant difference between the control group and the anti-miR-495 group *in vitro*. We used flow cytometry assays to identify whether this was due to induction of apoptosis; Annexin V-PI staining indicated higher apoptosis rates in miR-495 transfected cells (Figure 4B). Furthermore, Western blot was performed to measure the protein levels of Bcl-xl and Bax, which are key regulators of apoptosis. Our results showed that miR-495 over-expression raised the level of Bax and decreased the level of Bcl-xl (Figure 4C). To verify whether the proliferation inhibition

effect was dependent on HMGA2, we silenced the HMGA2 expression, and detected no proliferation inhibition effect of miR-495 on osteoblast (Figure 4D).

MiR-495 inhibits bone regeneration *in vivo*

As described, drill-hole injury operations were performed on the mice; miR-495 antisense oligonucleotides were administered to mice (7 mg/kg) [19] on days 0, 4, 7, 11, and 14 after the surgery. MiC (7 mg/kg) was injected as a control. Then 21 days later, the mice were sacrificed for microCT analysis. MicroCT images are shown in Figure 5A. Silencing miR-495 promoted bone regeneration. BV/TV, Tb.Th, and Tb.N were assessed according to microCT. Data indicated that the inhibition of miR-495 increased BV/TV, Tb.Th, and Tb.N (Figure 5B).
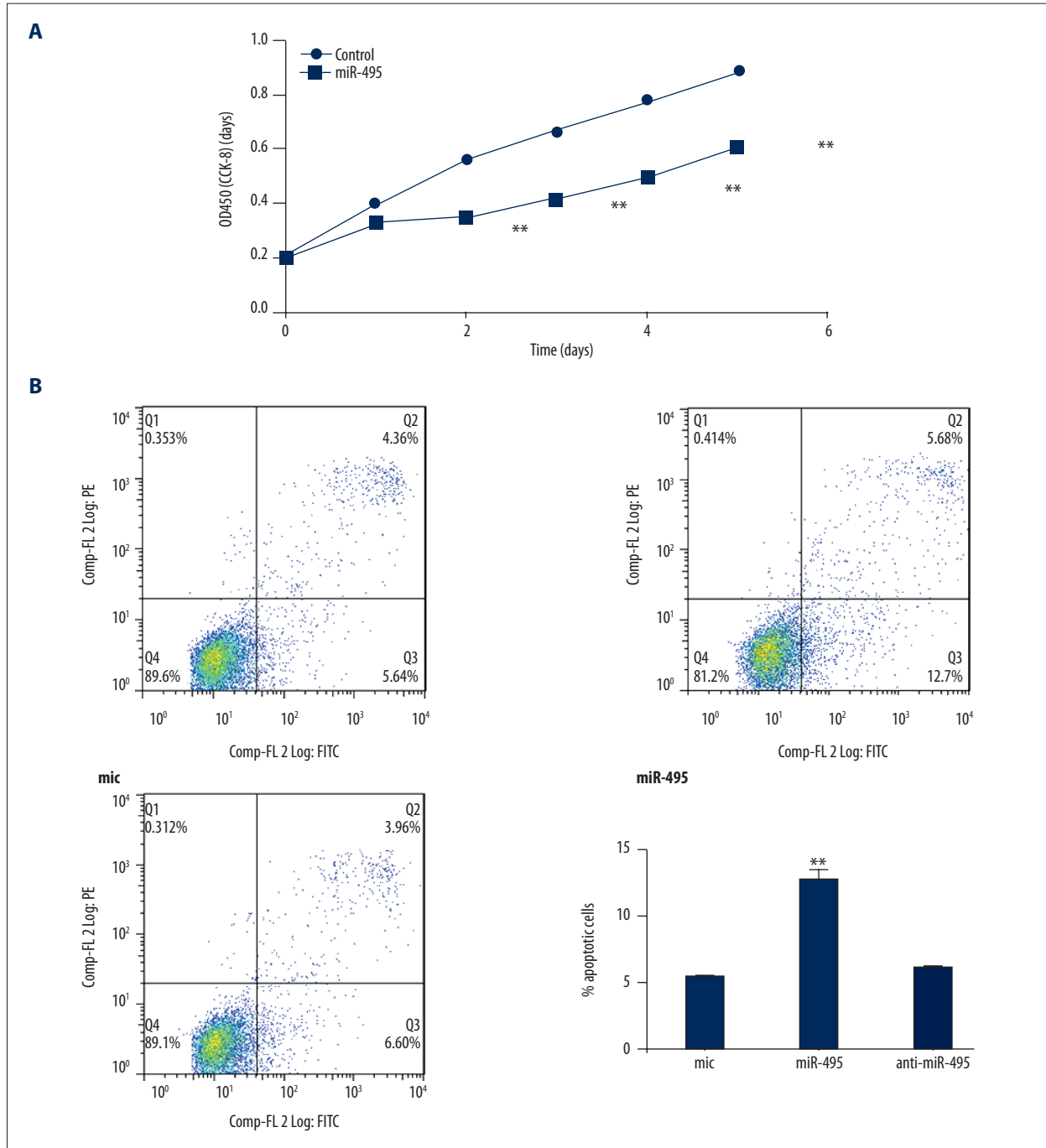
Discussion

New bone regeneration is vital in diverse common bone disorders, including trauma and osteoporosis. Although researchers have explored various treatment methods to overcome these conditions [22], there are almost no extremely effective therapies. In this study, we investigated a novel miRNA involved in osteoblast differentiation. From both *in vitro* and *in vivo* studies, we found that miR-495 suppressed bone formation while anti-miR-495 attenuated this effect. The miR-495 upregulation decreased the ALP activity and mineralization nodule formation and also downregulated osteogenic marker expressions such as RUNX-2, BMP-2, and Osterix. To further study the underlying mechanisms, we searched prediction tools to find potential targets of miR-495. We selected to focus our investigation on

3'UTR of HMGA2. We found that miR-495 upregulation inhibited luciferase activity. Using an apoptosis assay, we found that miR-495 induced osteoblast apoptosis by targeting HMGA2. We thus concluded that miR-495 inhibits bone regeneration via targeting HMGA2.

In recent years, miR-495 has been studied as a tumor suppressor gene. It has been reported that miR-495 suppresses the post-transcription of forkhead box C1 (FOXC1) and thus inhibits endometrial cancer progression [23]. Also, miR-495 inhibits the migration and invasion of gastric cancer cells via interacting directly with phosphatase of regenerating liver-3 (PRL-3) [24,25]. Similar results also have been found in non-small cell lung cancer [26], leukemia [27], and prostate cancer [28]. However, little has been studied on the role of miR-495 in osteoblast cells differentiation or bone regeneration. We observed in our study that miR-495 suppressed mice osteoblast differentiation and new bone regeneration. HMGA2,

This work is licensed under Creative Common Attribution-NonCommercial-NoDerivatives 4.0 International (CC BY-NC-ND 4.0)

4695

Indexed in: [Current Contents/Clinical Medicine] [SCI Expanded] [ISI Alerting System]
[ISI Journals Master List] [Index Medicus/MEDLINE] [EMBASE/Excerpta Medica]
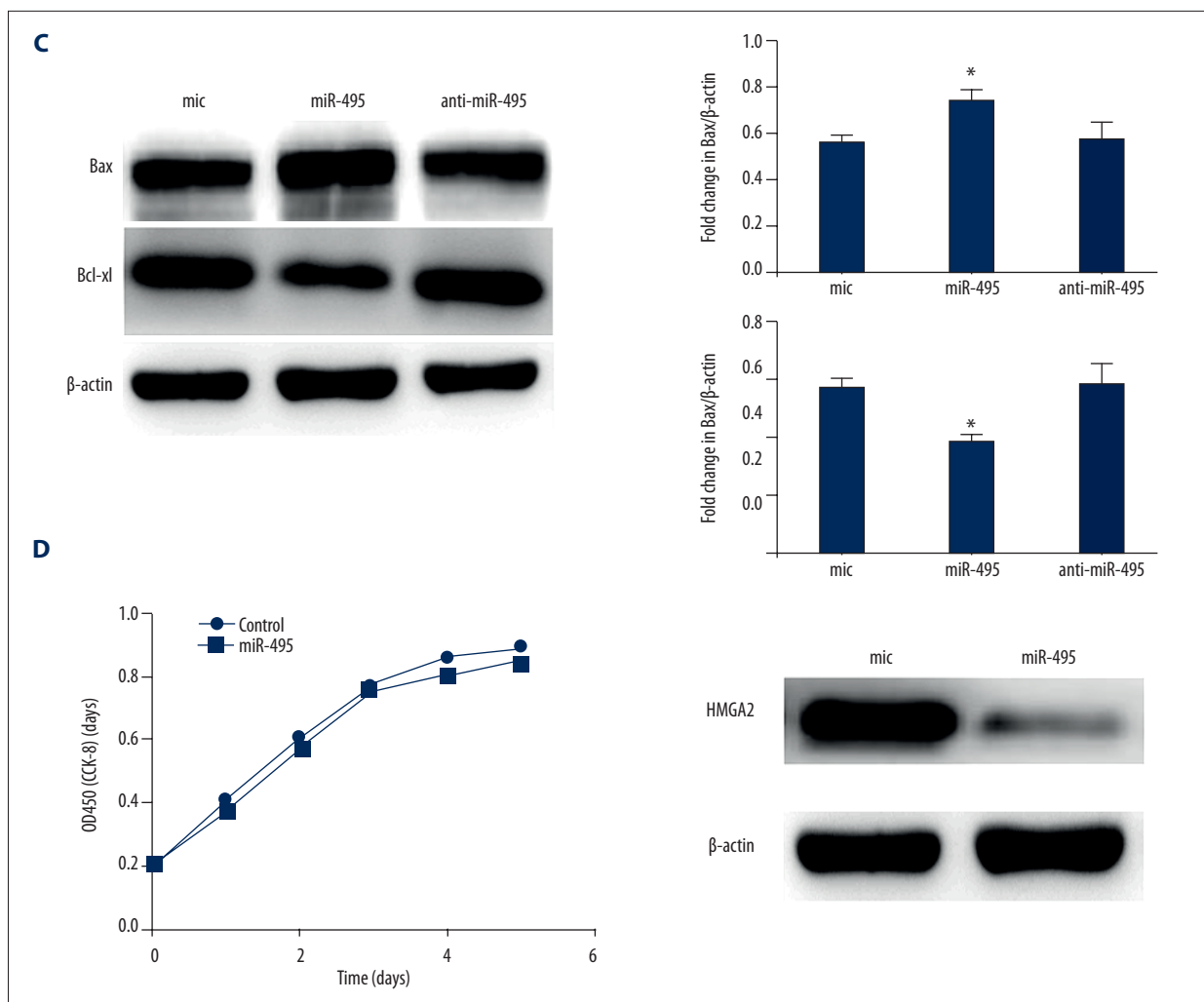[Chemical Abstracts/CAS] [Index Copernicus]

Figure 4. MiR-495 inhibits osteoblasts proliferation and promotes osteoblasts apoptosis. (**A**) Cells were transfected with miC or miR-495 and CCK-8 was performed to detect the proliferation. (**B**) Cells were grown to about 50% confluence and exposed to miC, miR-495 and anti-miR-495 for 24 hours. Flow cytometry was used to measure the apoptotic rate in different groups. (**C**) Cells were transfected with miC, miR-495, and anti-miR-495. Western blot analysis of Bcl-XL and Bax. Western blot of β-actin was included as a loading control. (**D**) Cells were silenced for HMGA2 and transfected with miC or miR-495. CCK-8 was used for detecting the proliferation of osteoblasts. ** *p*<0.01.

as a nuclear-binding protein, plays critical roles in cell proliferation and differentiation [29]. In various cancers, it is overexpressed [30]. In osteosarcoma, miR-106a-5p inhibits osteosarcoma cells proliferation, invasion, and migration by targeting HMGA2 [31]. In addition, silencing of HMGA2 by shRNAs inhibits the proliferation of bone marrow-derived mesenchymal stem cells (MSCs) [21]. However, there are controversial ideas about the role of HMGA2 in osteoblast differentiation. It was reported that let-7 promotes osteogenesis of MSCs *in vitro* and *in vivo* via repressing HMGA2 expression [32]. In this study, we illustrated, for the first time, that miR-495 restrained HMGA2 expression and thus promoted osteoblast apoptosis.

Conclusions

In conclusion, results from our study indicated that miR-495 negatively regulate osteogenesis by targeting HMGA2 expression which regulates the apoptosis of osteoblast cells. In addition, the inhibition of miR-495 functionally promotes osteoblast proliferation and accelerates bone regeneration *in vivo*. Hence, we suggest that targeting miR-495 might be a promising therapy for enhancing new bone regeneration.
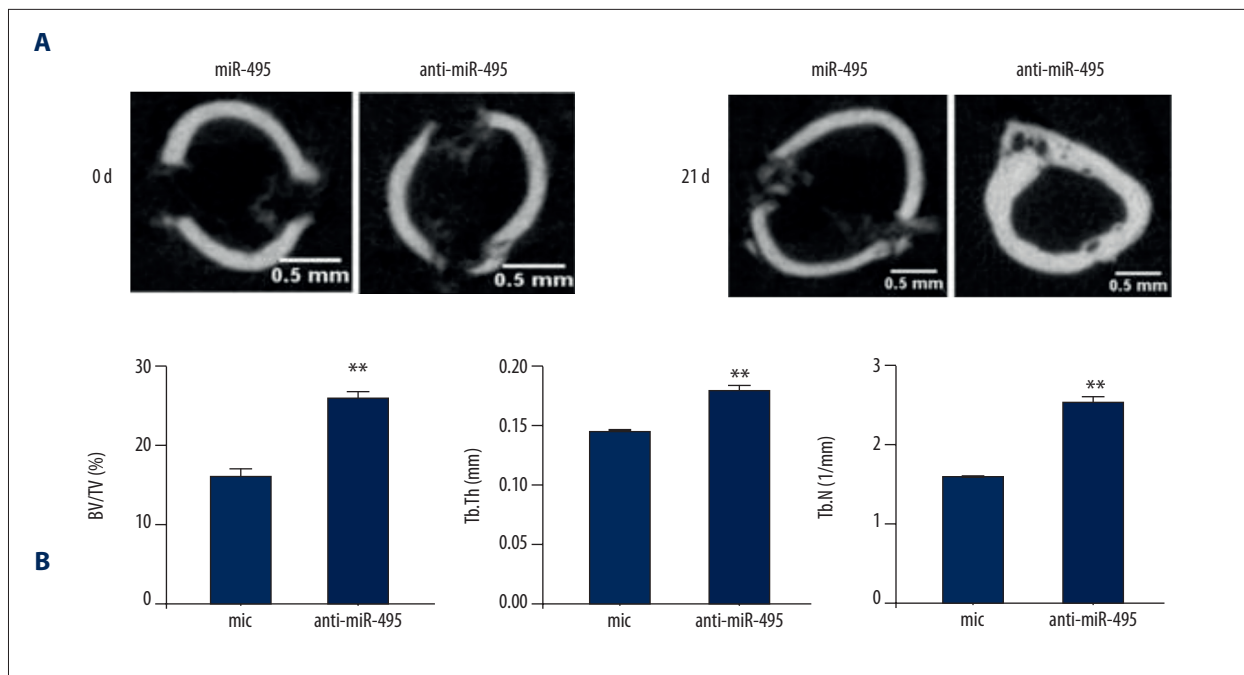
Conflict of interest

None.

Figure 5. MiR-495 regulates bone regeneration *in vivo*. (**A**) Representative micro CT images showing bone healing in each group. (**B**) Anti-miR-495 restores femoral microarchitecture showing bone volume fraction (BV/TV), Thickness of trabecularized spicules (Tb.Th) and trabecular number (Tb.N). All values represent means ±SD (n=8). ** *p*<0.01.

References:

1. Dong J, Cui X, Jiang Z, Sun J: MicroRNA-23a modulates tumor necrosis factor-alpha-induced osteoblasts apoptosis by directly targeting Fas. J Cell Biochem, 2013; 114: 2738–45

2. Hassan MQ, Maeda Y, Taipaleenmaki H et al: miR-218 directs a Wnt signaling circuit to promote differentiation of osteoblasts and osteomimicry of metastatic cancer cells. J Biol Chem, 2012; 287: 42084–92

3. Eskildsen T, Taipaleenmaki H, Stenvang J et al: MicroRNA-138 regulates osteogenic differentiation of human stromal (mesenchymal) stem cells *in vivo*. Proc Natl Acad Sci USA, 2011; 108: 6139–44

4. Bartel DP: MicroRNAs: Target recognition and regulatory functions. Cell, 2009; 136: 215–33

5. Inose H, Ochi H, Kimura A et al: A microRNA regulatory mechanism of osteoblast differentiation. Proc Natl Acad Sci USA, 2009; 106: 20794–99

6. Mencia A, Modamio-Hoybjor S, Redshaw N et al: Mutations in the seed region of human miR-96 are responsible for nonsyndromic progressive hearing loss. Nat Genet, 2009; 41: 609–13

7. Hughes AE, Bradley DT, Campbell M et al: Mutation altering the miR-184 seed region causes familial keratoconus with cataract. Am J Hum Genet, 2011; 89: 628–33

8. de Pontual L, Yao E, Callier P, Faivre L et al: Germline deletion of the miR-17 approximately 92 cluster causes skeletal and growth defects in humans. Nat Genet, 2011; 43: 1026–30

9. Vosa U, Vooder T, Kolde R et al: Identification of miR-374a as a prognostic marker for survival in patients with early-stage nonsmall cell lung cancer. Genes Chromosomes Cancer, 2011; 50: 812–22

10. Eyking A, Reis H, Frank M et al: MiR-205 and MiR-373 are associated with aggressive human mucinous colorectal cancer. PLoS One, 2016; 11: e156871

11. Chen JF, Murchison EP, Tang R et al: Targeted deletion of Dicer in the heart leads to dilated cardiomyopathy and heart failure. Proc Natl Acad Sci USA, 2008; 105: 2111–16

12. Wagschal A, Najafi-Shoushtari SH, Wang L et al: Genome-wide identification of microRNAs regulating cholesterol and triglyceride homeostasis. Nat Med, 2015; 21: 1290–97

13. Kureel J, John AA, Dixit M, Singh D: MicroRNA-467g inhibits new bone regeneration by targeting Ihh/Runx-2 signaling. Int J Biochem Cell Biol, 2017; 85: 35–43

14. Zhang Y, Gao Y, Cai L et al: MicroRNA-221 is involved in the regulation of osteoporosis through regulates RUNX2 protein expression and osteoblast differentiation. Am J Transl Res, 2017; 9: 126–35

15. Liu J, Li Y, Luo M et al: MicroRNA-214 inhibits the osteogenic differentiation of human osteoblasts through the direct regulation of baculoviral IAP repeat-containing 7. Exp Cell Res, 2017; 351: 157–62

16. Liu L, Liu M, Li R et al: MicroRNA-503-5p inhibits stretch-induced osteogenic differentiation and bone formation. Cell Biol Int, 2017; 41: 112–23

17. Bhargavan B, Singh D, Gautam AK et al: Medicarpin, a legume phytoalexin, stimulates osteoblast differentiation and promotes peak bone mass achievement in rats: evidence for estrogen receptor beta-mediated osteogenic action of medicarpin. J Nutr Biochem, 2012; 23: 27–38

18. Gautam AK, Bhargavan B, Tyagi AM et al: Differential effects of formononetin and cladrin on osteoblast function, peak bone mass achievement and bioavailability in rats. J Nutr Biochem, 2011; 22: 318–27

19. Kureel J, Dixit M, Tyagi AM et al: miR-542-3p suppresses osteoblast cell proliferation and differentiation, targets BMP-7 signaling and inhibits bone formation. Cell Death Dis, 2014; 5: e1050

20. Wang H, Sun Z, Wang Y et al: miR-33-5p, a novel mechano-sensitive microRNA promotes osteoblast differentiation by targeting Hmga2. Sci Rep, 2016; 6: 23170

21. Kalomoiris S, Cicchetto AC, Lakatos K et al: Fibroblast growth factor 2 regulates high mobility group A2 expression in human bone marrow-derived mesenchymal stem cells. J Cell Biochem, 2016; 117: 2128–37

22. Hu C, Zhang T, Ren B et al: Effect of vacuum-assisted closure combined with open bone grafting to promote rabbit bone graft vascularization. Med Sci Monit, 2015; 21: 1200–6

23. Xu YY, Tian J, Hao Q, Yin LR: MicroRNA-495 downregulates FOXC1 expression to suppress cell growth and migration in endometrial cancer. Tumour Biol, 2016; 37: 239–51

24. Li Z, Cao Y, Jie Z et al: miR-495 and miR-551a inhibit the migration and invasion of human gastric cancer cells by directly interacting with PRL-3. Cancer Lett, 2012; 323: 41–47

25. Li Z, Zhang G, Li D et al: Methylation-associated silencing of miR-495 inhibit the migration and invasion of human gastric cancer cells by directly targeting PRL-3. Biochem Biophys Res Commun, 2015; 456: 344–50

26. Chu H, Chen X, Wang H et al: MiR-495 regulates proliferation and migration in NSCLC by targeting MTA3. Tumour Biol, 2014; 35: 3487–94

27. Jiang X, Huang H, Li Z et al: MiR-495 is a tumor-suppressor microRNA downregulated in MLL-rearranged leukemia. Proc Natl Acad Sci USA, 2012; 109: 19397–402

28. Formosa A, Markert EK, Lena AM et al: MicroRNAs, miR-154, miR-299-5p, miR-376a, miR-376c, miR-377, miR-381, miR-487b, miR-485-3p, miR-495 and miR-654-3p, mapped to the 14q32.31 locus, regulate proliferation, apoptosis, migration and invasion in metastatic prostate cancer cells. Oncogene, 2014; 33: 5173–82

29. Park SM, Shell S, Radjabi AR et al: Let-7 prevents early cancer progression by suppressing expression of the embryonic gene HMGA2. Cell Cycle, 2007; 6: 2585–90

30. Wei JJ, Wu J, Luan C et al: HMGA2: a potential biomarker complement to P53 for detection of early-stage high-grade papillary serous carcinoma in fallopian tubes. Am J Surg Pathol, 2010; 34: 18–26

31. He QY, Wang GC, Zhang H et al: miR-106a-5p suppresses the proliferation, migration, and invasion of osteosarcoma cells by targeting HMGA2. DNA Cell Biol, 2016; 35: 506–20

32. Wei J, Li H, Wang S et al: let-7 enhances osteogenesis and bone formation while repressing adipogenesis of human stromal/mesenchymal stem cells by regulating HMGA2. Stem Cells Dev, 2014; 23: 1452–63